Journal of Alloys and Compounds 509 (2011) 4035–4040

Contents lists available at ScienceDirect

Journal of Alloys and Compounds

journal homepage: www.elsevier.com/locate/jallcom

One-dimensional growth of zinc oxide nanostructures from large micro-particles in a highly rapid synthesis

Shahrom Mahmud*

Nano Optoelectronic Research (NOR) Lab, School of Physics, Universiti Sains Malaysia, 11800 Minden, Pulau Pinang, Malaysia

ARTICLE INFO

Article history:
Received 8 November 2010
Received in revised form 2 January 2011
Accepted 3 January 2011
Available online 5 January 2011

Keywords:
Nanostructured materials
Oxide materials
Crystal growth
Rapid-solidification
Quenching

ABSTRACT

Large and irregularly-shaped zinc oxide (ZnO) micro-particles commonly found in a high-temperature vapor-phase process known as the catalyst-free combust-oxidized mesh (CFCOM) process, play a crucial role as nucleation hosts for ZnO one-dimensional (1D) nanostructures, especially nanometric wires and rods. Nanowires and nanorods tend to grow from the hillocks of the large micro-particles whereby these hillocks serve as nucleation sites for the acicular structures. Nanowires with aspect ratios exceeding 5 are the most common 1D structures that grow from pillar-like hillocks, while triangular hillocks are probable nucleation hosts for nanorods. The ZnO nanostructures possess a polycrystalline nature with photoluminescent emission in the UV band-edge and visible regimes. A novel and non-destructive electrical resistance measurement method is introduced in that the 1D ZnO nanostructures exhibited very high GΩ resistance that is over five times higher than that of commercial ZnO. A growth model is proposed to offer a probable explanation for the fascinating rapid growth of 1D nanostructures originating from large ZnO micro-particles. The ZnO particles in this work were synthesized using 5-ton industrial furnaces via a university-industry joint effort.

1. Introduction

The rich structural diversity of zinc oxide (ZnO) has attracted immense research activity especially due its potential and current applications in UV/blue LEDs, piezoelectric devices, transparent electronics, chemical nanosensors, spin electronics, optoelectronic displays, UV lasing, electro-optical switches, varistors, ferrites, ceramics, rubber vulcanization, pharmaceuticals, cosmetics and textiles [1–6]. Moreover, ZnO can be synthesized in many shapes resembling wires, rods, tubes, spirals, rings, bows, belts, helixes, tripods, tetrapods, combs, propellers, drums, polyhedrons, discs, cages, flowers, stars, boxes, mallets and plates [1,7–11]. The diverse ZnO nanostructure species are synthesized via several techniques, such as gas phase synthesis, vapor–solid (VS) process, vapor–liquid–solid (VLS) reaction, metalorganic vapor-phase epitaxy, thermal chemical vapor deposition, molecular beam epitaxy (MBE), thermal annealing and catalyst-free combust-oxidized mesh (CFCOM) processing [1,2,12].

Most of the annual global ZnO production of over 1.2 million tons is manufactured using the French process, a century-old technology. Due to the catalyst-free nature and rapid oxidation process, it can be known as a catalyst-free combust-oxidized (CFCO) method [9,10]. Fig. 1(a) shows a photograph of industrial ZnO furnaces employing the CFCO process. Each furnace is made up of a graphite crucible that is placed inside a firebrick housing. Zinc ingots are transferred into the crucible for melting and vaporization. Zinc melts at 419.5 °C with heat of fusion 7.39 kJ/mol and boils at 907 °C with heat of vaporization 114.8 kJ/mol; and at furnace temperature of 1000–1500 °C, zinc vapor is pressurized inside the crucible to an estimated value of 0.2–1.1 MPa [11–13]. Once the crucible lid is removed, the pressurized zinc gas escapes at a calculated velocity of Mach 0.1–0.5 and it is instantly oxidized by ambient air. Due to high temperatures and a high level of supersaturation, crystal growth occurs almost instantly to form a coalescence of ZnO aggregates of primary particles. This is shown in Fig. 1(b) in which various species of nanostructures (rods, wires, plates, mallets, drums, boxes, etc.) can be seen to coexist and codiffuse even in a small region of less than 1 μm^3, giving rise to the notion of nanoscopic inhomogeneity [9–12]. Aggregates of primary ZnO nanoparticles are typical entities of the commercial French process ZnO in that the aggregates possess sizes ranging from a few microns up to several tens of microns.

The high cost of nanometric ZnO (nano ZnO) has been the biggest hindrance to its wider applications in the rubber, varistor, textile and catalysis industries. A modified French process, known as the catalyst-free combust-oxidized mesh (CFCOM) process, offers a low-cost alternative to the large scale fabrication of nanometric ZnO with a capacity exceeding 1 kg/h [12]. However, the growth mechanism of the CFCOM process is still unclear, and there is

* Tel.: +60 12 5710976; fax: +60 4 6579150.
E-mail address: shahromx@usm.my

0925-8388/$ – see front matter © 2011 Elsevier B.V. All rights reserved.
doi:10.1016/j.jallcom.2011.01.013

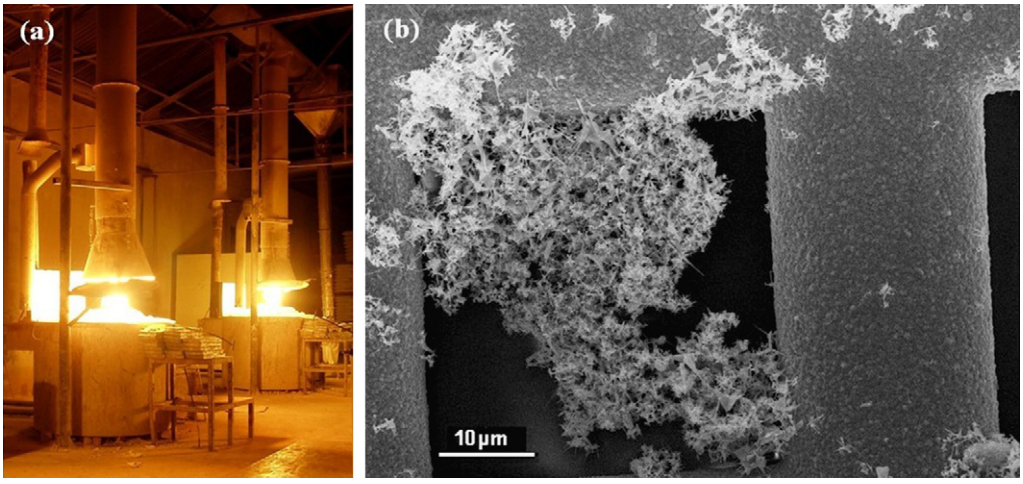

Fig. 1. (a) Photo of ZnO industrial furnaces used in this work, and (b) FESEM micrograph of ZnO particles trapped on copper grid with carbon layer.

very little literature about it. A good understanding of this new process is crucial in designing a better technique capable of selectively synthesize the growth of a preferred morphology at industrial capacities. In the CFCOM process, the ZnO primary nanoparticles are more acicular than that of the ZnO French process, and the aggregates form sprawling colonies that span many tens of microns as shown in Fig. 1(b). It is also found that the CFCOM process also produces irregularly-shaped ZnO particles of several microns and these relatively large particles are of prime interest in the present study that investigates the role of these micro-particles in the development of one-dimensional nanostructures of ZnO. Once a convincing growth mechanism is well understood, effort can be made to upgrade the century-old French process technology for a promising mass production of high quality and cheap one-dimensional (1D) ZnO nanoparticles.

2. Experiment

ZnO particles were synthesized in a ZnO factory using 5-ton industrial furnaces as shown in Fig. 1(a). About 250 kg of zinc ingots (Zinifex 99.995% purity) were charged into the furnace crucible. The furnace was heated to melt and vaporize the zinc metal. As zinc vapor exited the crucible, it was instantly oxidized into ZnO that was sucked/transported via a 100 m long ducting to the baghouse. With the help of a pyrometer (Raytek 3i 1 M), the exit temperature of the escaping zinc gas flow was observed to be about 1280–1300 °C. Safety measures such as wearing fire-resistant apparels (gloves, suit and hood) were taken during the experiment due to hazardous open flame radiation. The CFCOM process began by placing a 16 cm × 16 cm steel wire mesh sieve (Tyler 20) about 1 cm above the orifice of the ZnO furnace. At this position, the steel sieve was instantly heated to a whitish flame as hot zinc vapor gushed out from the crucible at supersonic speed. Some zinc vapor was captured on the mesh surfaces of the steel sieve. After 10 s of capturing time, the steel sieve was removed for natural air quenching during which one-dimensional (1D) ZnO nanostructures were grown. As soon as the hot steel sieve was removed from the furnace, it turned from a yellowish to a reddish flame in about 3–4 s. The sieve temperature was about 700 °C when its reddish emission disappeared and it took another 5–6 s to reach a temperature of about 400 °C. The powder on the steel mesh is scrapped off with a spatula. The as-grown ZnO was analyzed with a LEOSupra50VP field emission scanning electron microscope (FESEM) equipped with energy dispersive spectrometry (EDS), a Panalytical X'pert Pro Mrd Pw3040 X-ray diffractometer, a PhillipsCM12 transmission electron microscope (TEM), and a Jobin Yvon Horiba HR800UV photoluminescent (PL) spectroscopy unit.

A novel non-destructive method was employed in order to make ZnO pellets for electrical resistance measurement. In a 300 cm^3 beaker, 50 g ZnO powder was mixed with 200 cm^3 distilled water and about 3 cm^3 of the mixture was transferred, using a syringe, into a water-resistant paper cup with a diameter of 13 mm and height of 25 mm. The filled cup was left for room-temperature drying for two days until the powder settled down to form a pellet. The process was repeated to make two dozen pellets. Heavier agglomerates settled earlier than smaller particles that formed a thin crust of about 0.8 mm on the top surface of the pellet whereby the crust was rich in undamaged primary nanoparticles. Electrical measurement performed on the surfaces of the pellets using a Keithly 251 (model 82-138) I-V tester. For electrical measurement, a pair of electrode-pin probes was slightly embedded into the top surface of the ZnO pellet with a penetration of about 0.5 mm. The probe gap distance was set at about 3 mm and it was found that no significant electrical change was observed if the probe gap was within 2–5 mm. Electrical measurements were done in dark conditions. It was found that current-triggering was the stable mode for obtaining a voltage–current (*V–I*) spectrum instead of the normal voltage-triggering mode. For PL and electrical comparison, pellets from commercial ZnO were also prepared from the rubber grade (White seal grade from Approfit) and Pharma grade (Pharma grade from Approfit).

3. Results and discussion

3.1. Crystallography and morphology

As-grown ZnO powder, obtained from the steel wire mesh, was found to have an off-white appearance. The FESEM micrograph in Fig. 2(a) shows a sprawling colony of micro-particles consisting of chainlike aggregates of primary particles. Nanorods and nanowires appeared to have grown out of the micro-particles and this phenomenon is also shown by the all the micrographs of Fig. 2. The acicular nanostructures have diameters of 10–100 nm and lengths of 200–2000 nm. The big dimensional variations among the structures indicate a synthesis with highly unstable growth parameters. Most of the one-dimensional (1D) structures appear to be nanowires that can be classified as those possessing an aspect ratio (length/diameter) exceeding 5, based on the empirical ZnO growth equation reported earlier [10]. These 1D nanostructures can be regarded as the primary particles of aggregates [14]. Aggregation of primary particles is currently one of the major setbacks of gas phase syntheses, such as the CFCOM process, and the aerosol and flame spray pyrolysis, because aggregation can reduce bulk specific surface area and filler homogeneity in composites. The selected area electron diffraction (SAED) ring pattern of Fig. 2(b) confirmed the polycrystalline nature of the as-grown ZnO powder in that the SAED diffraction rings can be assigned to ZnO crystal indices of (0 0 0 2), (1 0 $\bar{1}$ 1), (1 1 $\bar{2}$ 0), (1 1 $\bar{2}$ 2), (2 0 $\bar{2}$ 2) and (1 0 $\bar{1}$ 4). Interestingly, the growth of nanowires from ZnO micro-particles can be made into "nano art" as shown by the unique crystallographic formation of Fig. 2(e) and (f) that possess striking resemblances of a mousedeer and rocket, respectively, giving rise to the names ZnO nanodeer and nanorocket. These intriguing "nano art" formations were most probably coincidental works of nature. And it would be even more intriguing to realize that the rapid synthesis of the CFCOM process, lasting less than 1 min (or subminute), was able to produce nanowires in a large scale.

EDS area scan done on as-grown ZnO is posted in Fig. 2(c) and the data implicates a high level of ZnO purity since only O and Zn peaks are prominently visible whereby the O peak is observed at 0.52 keV

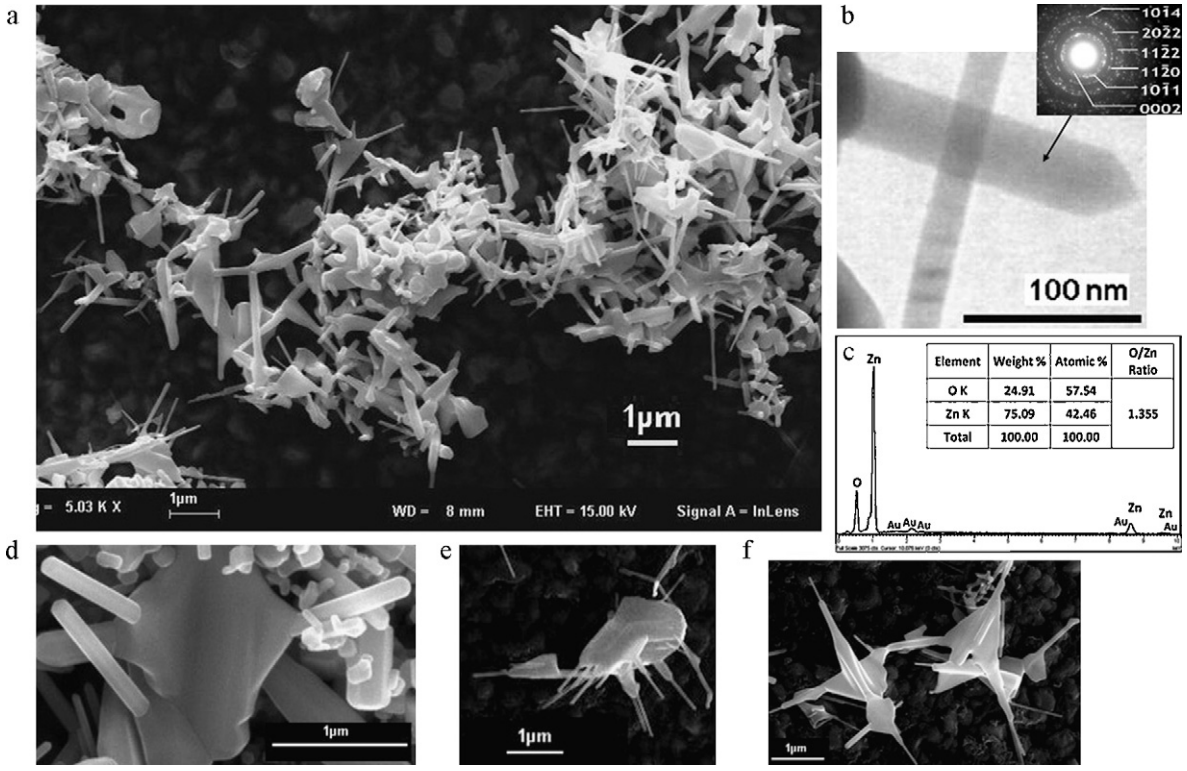

Fig. 2. (a) FESEM micrograph of a sprawling colony of ZnO particles, (b) TEM micrograph of ZnO 1D nanostructures showing SAED ring patterns, (c) EDS spectrum, (d) FESEM micrograph of ZnO 1D structures, and fascinating ZnO structures resembling (e) deer and (f) rocket.

critical energy and the Zn peaks are observed at 1.01 keV, 8.63 keV and 9.57 keV. Non-related peaks refer to a gold (Au) coating, while the peak at 0.282 keV refers to a carbon (C) film on the TEM copper grid used to capture the ZnO particles. The absence of impurities in the EDS spectrum indicates that the CFCOM synthesis was free from impurities. The relative atomic oxygen-to-zinc (O/Zn) ratio is 1.355 which is almost similar to the ones reported in our earlier work [9] and this O/Zn ratio value can indicate near complete oxidation of the synthesis.

The polycrystalline nature of the as-grown ZnO is confirmed by the XRD spectrum in Fig. 3 that shows diffraction peaks of JCPDS card 36-1451 that is referring to wurtzite ZnO. The XRD diffraction peaks also coincide with the TEM-SAED diffraction rings of Fig. 2(b) that confirms the presence of ZnO indices referring to XRD peaks at 34.3° (0 0 0 2), 36.1° (1 0 $\bar{1}$ 1), 56.5°(1 1 $\bar{2}$ 0),67.8° (1 1 $\bar{2}$ 2) and 77.1° (2 0 $\bar{2}$ 2). The major XRD diffraction peaks of (1 0 $\bar{1}$ 0), (0 0 0 2) and (1 0 $\bar{1}$ 1) appear strong and narrow, suggesting a high level of crystallinity of the as-grown powder. The polycrystalline structure was the result of high growth temperatures exceeding 1000 °C, short growth time and non-uniform crystallization conditions of the CFCOM technology. As a result, huge stress developed during growth and the resulting strain mismatch was relaxed by the grain boundaries of the polycrystals. The large stress also suppressed the alignment of nanostructures thereby preventing the formation of single crystalline structures [1,12,14].

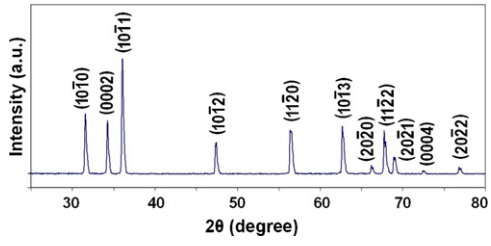

Fig. 3. XRD spectrum for ZnO from the CFCOM method.

3.2. Electrical–optical analyses

Electrical measurement was done on ZnO pellets that were prepared via a new non-destructive method as explained in Section 2. ZnO pellets were also prepared for commercial ZnO namely Pharma grade and White grade, whereby the as-grown ZnO was labeled as CFCOM ZnO. Fig. 4(a) and (b) shows FESEM micrographs of Pharma and White ZnO grades, respectively, whereby ZnO rods with hexagonal cross-section (inset of Fig. 4(a)) are commonly found in Pharma ZnO. For White ZnO, rectangular-like structures are normally observed and the structures are shown in Fig. 4(b). During electrical measurement, a pair of electrode-pin probes was slightly embedded into the top surface of the ZnO pellet with a penetration of about 0.5 mm as illustrated by the inset photograph of Fig. 5(a). Since the voltage–current (*V–I*) spectra of Fig. 5(a) are not really linear, the *best-linear-fit* method was employed to obtain average resistance referring to the slope of the spectra. From the current-triggered *V–I* spectra, it is evident that CFCOM ZnO possesses the highest electrical resistance of about 5.28 GΩ if compared to that of Pharma (1.05 GΩ) and White (0.21 GΩ). Since pure and undoped ZnO normally exhibits GΩ cm resistivities [15], the GΩ resistances from the three samples are comparable with that obtained from other methods.

The very large resistance of CFCOM ZnO (five times that of commercial ZnO) can be attributed to the high concentration of structural intrinsic defects that exist in the one-dimensional nanostructures as indicated by the abnormally large visible photoluminescent (PL) emission in the 450–600 nm broad band

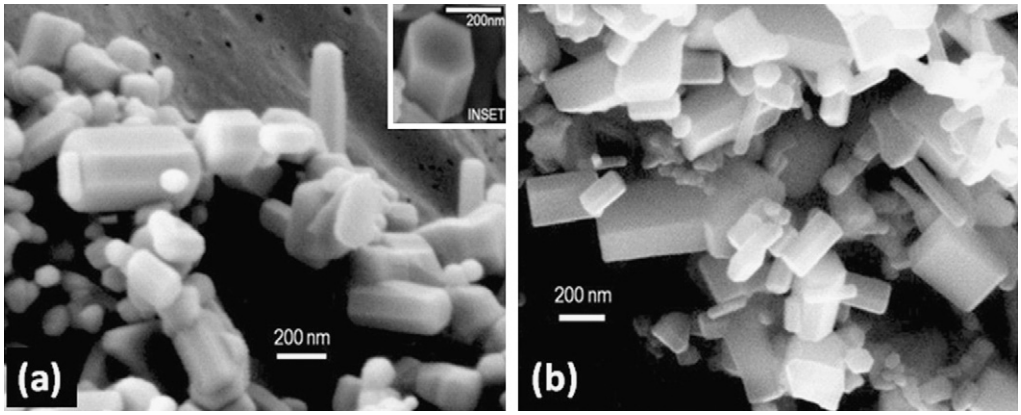

Fig. 4. FESEM micrographs of (a) Pharma ZnO, and (b) White ZnO.

(centering at 503 nm) as shown in Fig. 5(b). Karali et al. and Dakhloui et al. reported that the probable origins of the broad blue-green-yellow-orange PL emission were oxygen and/or zinc vacancies ($V^{\bullet}_{O}$, $V^{2\bullet}_{O}$, V'_{Zn} and $V^{2'}_{Zn}$) [6,16] that can serve as charge trappers. Trapping of charges is known to be the underlying cause of the formation of huge potential barriers against current flow resulting in GΩ range resistance. The other samples (Pharma and White) also exhibited similar PL emission but with much lower intensities and centering at about 533 nm. The relatively lower visible PL emission (about three times lower) of Pharma and White specimens may explain the relatively lower electrical resistances reported in Fig. 5(a) in that the concentration of charge trappers may be much smaller than that of CFCOM ZnO.

The real origins of the PL visible bands have been a decade-long debate and no common agreement is achieved. The broad and intense blue–green–yellow–orange PL emission band of the as-grown ZnO (CFCOM ZnO) suggests the presence of a high concentration of structural defects that are actually expected for a rapid synthesis with a rapid quenching step such as the CFCOM process. The sharp and prominent UV emission peak at about 391 nm indicates a bulk band gap of about 3.17 eV for CFCOM ZnO, and it refers to free-exciton recombination via an exciton-exciton collision process corresponding to a direct band gap transition of ZnO at room temperature [1,2]. From Fig. 5(b), CFCOM ZnO seems to exhibit a much stronger photocatalysis at the band-edge UV band if compared to that of the commercial samples (Pharma and White), and this very intense UV emission of CFCOM ZnO may be attributed to the high concentration of nanowires that are known to be strong emitters of UV light [1,7].

3.3. Crystal growth

The formation of hillocks on ZnO micro-particles was driven by the natural lowering of the free energy in systems [2,4], whereby ZnO particles formed hillocks to lower their overall free energy. Some hillocks resembled hills with triangular protrusions, while others resembled well-formed pillars as illustrated by the FESEM micrographs in Fig. 6(a) and (b). A well-formed ZnO pillar can be seen at the head of one nanorocket shown in Fig. 2(f). It was probable that the pillars were the matured version of hillocks as they formed with time.

The tips of hillocks can offer surfaces with low activation energy for nucleation [17] such that the tip surfaces can serve as preferred attachment sites for ZnO nucleation. Since the free energy of an atom reduces once it attaches to a surface and since a system will naturally lower its energy by every possible route [1,17], more atoms attached on the tip surfaces of hillocks and pillars. Rapid 1D growth could have taken place during the quenching stage of the CFCOM process due to the higher availability of oxygen from ambient air combined with lower growth temperature that offered the best conditions for the growth of acicular ZnO structures characterized by ±(0 0 0 2) crystal planes [2–4]. Since it is known that the (0 0 0 2) plane possesses the highest surface energy due to its polarized O^{2-}-terminated surface, it has the highest growth rate among all ZnO crystal planes [4,5]. Therefore, long acicular structures (rods and wires) grew during the quenching phase, as shown by the micrographs of Figs. 2 and 6.

Another notable observation is that the acicular nanostructures, grown from the pillars, possess much higher aspect ratios well

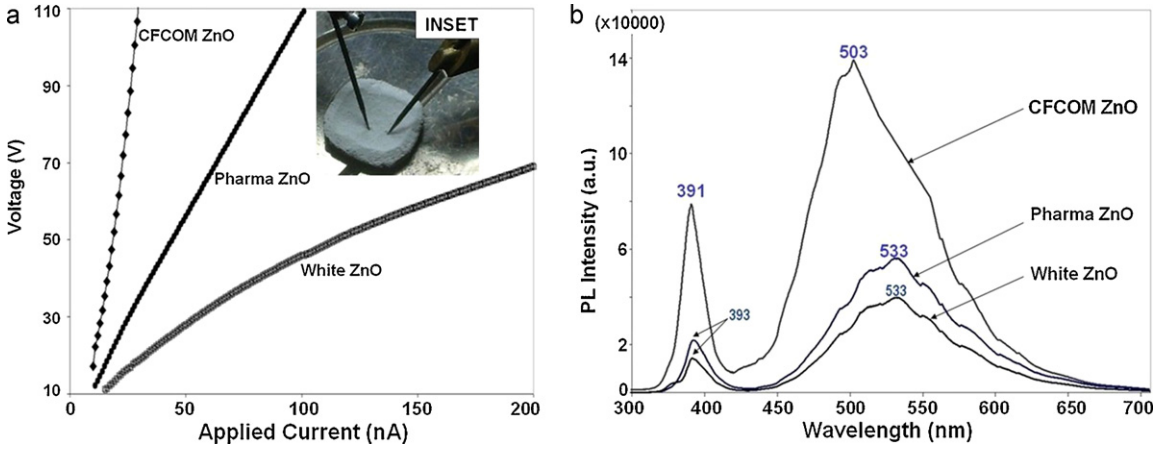

Fig. 5. (a) Voltage–current spectra, and (b) Photoluminescence spectra of ZnO samples.

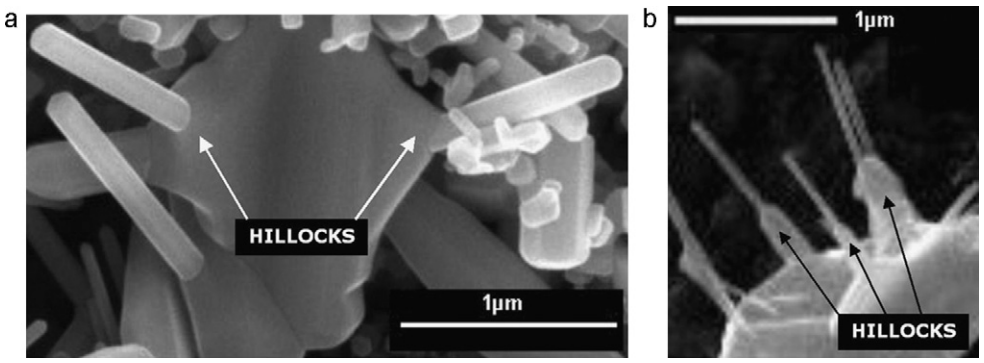

Fig. 6. (a) Triangular hillocks of one ZnO particle, and (b) pillar-like hillocks.

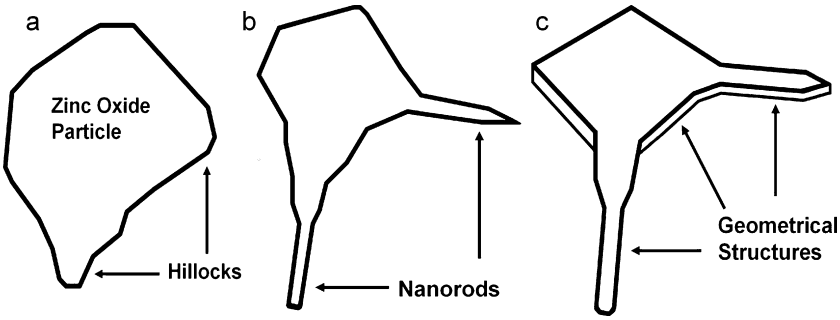

Fig. 7. Schematic diagram for 1D growth from ZnO particle showing (a) hillock formation, (b) acicular growth from hillocks and (c) geometrical transformation of ZnO particle.

exceeding 5 if compared to that grown from triangular hillocks, as shown in Fig. 6. From the micrograph in Fig. 6(b), it is evident that the pillar tips are tapered, perhaps during quenching onset, and the tapering resulted in smaller tip surfaces that served as smaller nucleation site surfaces conducive for the growth of high aspect ratio structures such as nanowires. On the other hand, lower aspect ratio structures (nanorods) grew from triangular hillocks as shown in Fig. 6(a). Therefore, the type of hillocks (triangular hills or pillars) can determine the type of acicular nanostructures (rods or wires) that resulted during secondary growth.

The nanorocket micrograph of Fig. 2(f) also presents an interesting observation for the ZnO micro-particles that are more structured with flat sheet geometry combined with perpendicular pillar-wire alignment. The micro-particle could have undergone structural transformation from an irregular shape to a more geometrical one that possesses lower surface energy.

3.4. Proposed growth model

Based on the discussion in the previous Section 3.2, a growth model is proposed for the unique growth of 1D ZnO nanostructures from ZnO micro-particles in the subminute process of CFCOM technology. The proposed growth model is presented in Fig. 7. During the CFCOM process, when the steel wire mesh sieve is placed just above the crucible orifice, ZnO micro-particles are formed. By the natural lowering of free energy of systems [2,4], hillocks are formed as shown in Fig. 7(a). Early formation of hillocks resembles triangular hills after which they transform into pillar-like hillocks. The hillock tips serve as nucleation host surfaces with low activation energy making them the preferred attachment sites for ZnO nucleation.

The quenching stage of the CFCOM process represents the secondary growth during which acicular structures grow very rapidly along (0 0 0 2) direction. The preferred morphology (rods or wires) depends on the hillock type from which the acicular structures grow. As shown in Fig. 6(b), pillar-like hillocks experience a tapering process during the onset of quenching resulting in smaller tip surfaces from which higher aspect ratio structures (nanowires) grow. Lower aspect ratio structures (nanorods) tend to grow from the larger tip surfaces of triangular-like hillocks.

During quenching, the ZnO micro-particles can experience a structural transformation into a flat like geometry that possesses lower surface energy as illustrated in Fig. 7(c).

4. Conclusion

A new growth mechanism of 1D ZnO nanostructures is presented in order to provide better insight for the growth of polycrystalline ZnO nanorods and nanowires originating from the hillocks of irregularly-shape micro ZnO particles that are synthesized via the ultra fast CFCOM process. The selective growth of morphology (rods or wires) very much depends on the type of hillock (triangular-like or pillar-like) from which the structures grow. This new growth model can be used to design better furnaces to selectively maximize the formation of pillar-like hillocks that serve as nucleation hosts for ZnO nanowires. The high purity and polycrystalline ZnO acicular nanostructures are found to possess structural defects that may be the underlying cause for visible PL emission and very large electrical resistance. The unique defect-induced properties can find potential applications in photonics and photocatalysis that operate in the UV and visible EM range. It is believed that the century-old French process can be upgraded via the CFCOM route to mass produce high quality and cheap ZnO nanoparticles possessing a polycrystalline nature and functional optical characteristics.

Acknowledgement

This work is supported by an incentive grant (304/JPNP/600004) from Universiti Sains Malaysia. I acknowledge the priceless assis-

tance from Mohd Zamzam Zakaria from Approfit Zinc Oxide Manufacturing Co. Ltd. for factory experiments. Assistance from USM electron microscopy unit and NOR lab is also acknowledged.

References

[1] H. Morkoc, U. Ozgur, Zinc Oxide: Fundamentals Materials and Device Technology, first ed., Wiley-VCH Verlag GmbH, 2009.
[2] R. Wahab, S.G. Ansari, Y.S. Kim, M.A. Dar, H.S. Shin, J. Alloys Compd. 461 (2008) 66–71.
[3] H.F. Lin, S.H. Liao, C.T. Hu, J. Cryst. Growth 311 (2009) 1378–1384.
[4] Z.L. Wang, X.Y. Kong, Y. Ding, P. Gao, W.L. Hughes, R. Yang, Y. Zhang, Adv. Funct. Mater. 14 (2004) 943–956.
[5] S.J. Pearton, W.H. Heo, M. Ivill, D.P. Norton, T. Steiner, Semicond. Sci. Technol. 19 (2004) R59.
[6] T. Karali, N. Can, L. Valberg, A.L. Stephanov, P.D. Townsend, Ch. Buchal, R.A. Ganeev, A.I. Ryasnyansky, H.G. Belik, M.L. Jessett, C. Ong, Physica B 363 (2005) 88–95.
[7] Z.L. Wang, Mater. Today 7 (2004) 26–33.
[8] A. Umar, S. Lee, Y.H. Im, Y.B. Hahn, Nanotechnology 16 (2005) 2462–2468.
[9] S. Mahmud, M.J. Abdullah, J. Chong, A.K. Mohamad, M.Z. Zakaria, J. Cryst. Growth 287 (2006) 118–123.
[10] S. Mahmud, M.J. Abdullah, J. Fiz. Mal. 27 (2006) 77–79.
[11] S. Mahmud, M.J. Abdullah, M.Z. Zakaria, Synth. React. Inorg. Met-Org. Nanomet. Chem. 35 (2006) 118–123.
[12] S. Mahmud, M.J. Abdullah, Solid State Sci. Technol. 15 (2007) 108–115.
[13] D.R. Lide, CRC Handbook of Chemistry and Physics, 87th ed., CRC, 2002.
[14] T. Tani, L. Madler, S.E. Pratsinis, J. Nanopart. Res. 4 (2002) 337–343.
[15] V.A. Karpina, V.I. Lazorenko, C.V. Lashkarev, V.D. Dobrowolski, L.I. Kopylova, B.A. Baturin, S.A. Pustovoytov, A.J. Karpenko, S.A. Eremin, P.M. Lytvyn, V.P. Ovsyannikov, E.A. Mazurenko, Cryst. Res. Technol. 39 (2004) 980–992.
[16] A. Dakhlaoui, M. Jendoubi, L.S. Smiri, A. Kanaev, N. Jouini, J. Cryst. Growth 311 (2009) 3989–3996.
[17] R.W. Kelsall, I.W. Hamley, M.M. Geoghegan, Nanoscale Science and Technology, John Wiley & Sons Ltd, Chichester UK, 2005.